International Journal of Non–Linear Mechanics 165 (2024) 104817

Contents lists available at ScienceDirect

International Journal of Non-Linear Mechanics

journal homepage: www.elsevier.com/locate/nlm

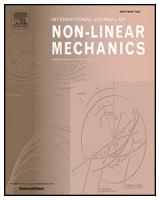

Seismic reliability analysis of nonlinear structures by active learning-based adaptive sparse Bayesian regressions

Atin Roy [a,*], Subrata Chakraborty [b], Sondipon Adhikari [a]

[a] James Watt School of Engineering, The University of Glasgow, Glasgow, G12 8QQ, United Kingdom
[b] Department of Civil Engineering, Indian Institute of Engineering Science and Technology, Shibpur, Howrah, India

ARTICLE INFO

Keywords:
Seismic reliability analysis
Nonlinear time history analyses
Sparse Bayesian regression
Adaptive sampling
Active learning
Monte Carlo simulation

ABSTRACT

The Monte Carlo simulation (MCS) technique is quite simple in concept and the most accurate for seismic reliability analysis (SRA) of structures involving nonlinear seismic response analysis, considering the effect of the stochastic nature of earthquakes and the uncertainty of various structural parameters. However, the approach needs to execute several repetitive nonlinear dynamic analyses of structures. The metamodeling technique has emerged as a practical alternative in such a scenario. In SRA, the dual metamodeling approach is typically adopted to deal with the stochastic nature of earthquakes following a lognormal seismic response assumption. In contrast, a direct metamodeling approach of SRA can avoid such prior assumptions. Adaptive training near the limit state is important in the metamodeling-based SRA. However, its implementation is quite challenging for SRA due to the record-to-record variation of earthquakes. In this context, an adaptive sparse Bayesian regression-based direct metamodeling approach is developed for SRA, where an active learning-based algorithm is proposed for adaptive training of metamodels for approximating nonlinear seismic responses. As the sparse Bayesian regression is computationally faster than Kriging due to the sparsity involved in sparse Bayesian learning, the overall performance of the proposed approach is expected to be better than the adaptive Kriging-based SRA approach. The effectiveness of the proposed approach is illustrated by numerical examples.

1. Introduction

Seismic risk assessment is a fundamental process used to evaluate the potential impact of earthquakes on structures, infrastructure, and communities. As natural phenomena, earthquakes pose significant threats to human safety, property, and economic stability. By analysing and quantifying the risks associated with seismic events, engineers, planners, and policymakers can make informed decisions to mitigate potential hazards and improve the resilience of communities and structures. The assessment involves a systematic analysis of various factors, including the random nature of earthquakes, uncertainties in parameters characterising nonlinear structural behaviour, and the seismic hazard of a particular region. It aims to estimate the probability of damage or failure of a structure under specific earthquake scenarios and hazard levels. By understanding the potential consequences of seismic events, appropriate measures can be taken to enhance building codes, retrofit existing structures, develop emergency response plans, and allocate resources effectively. Researchers have developed several approaches to estimate the reliability of nonlinear structures subjected to stochastic ground motions [1–3]. In fact, the performance-based earthquake engineering (PBEE) [4] approach has emerged to focus on designing structures to meet specific performance objectives under various earthquake scenarios. Seismic risk assessment is crucial in PBEE by providing valuable information to establish performance criteria and optimise designs.

Seismic reliability analysis (SRA) is a specialised methodology used to assess the probability of failure or damage to a structure when subjected to seismic forces. It is an essential component of seismic risk assessment and PBEE, providing valuable insights into the structural performance under various earthquake scenarios. The primary objective of SRA is to evaluate the reliability of a structure involving nonlinear seismic response analysis considering the uncertainties in material properties, geometric dimensions, and other factors that influence its behaviour during an earthquake. Unlike traditional deterministic methods, which assume fixed values for all parameters, SRA considers the inherent variability and randomness associated with earthquakes and structural responses. In classical random vibration theory, SRA typically models earthquakes as a stochastic process and solves the associated outcrossing problem. Typically, linear random vibration an-

* Corresponding author.
E-mail addresses: Atin.Roy@glasgow.ac.uk (A. Roy), schak@civil.iiests.ac.in (S. Chakraborty), Sondipon.Adhikari@glasgow.ac.uk (S. Adhikari).

https://doi.org/10.1016/j.ijnonlinmec.2024.104817
Received 12 October 2023; Received in revised form 28 March 2024; Accepted 17 June 2024
Available online 21 June 2024

alyses are conducted in the frequency domain using averaged power spectra from various sources. This provides insight into maximum elastic structural responses but underestimates the variabilities in the response quantities compared to that obtained by analyses using recorded accelerograms. Additionally, the frequency domain approach derived from classical random vibration theory is inadequate for SRA within the PBEE framework, which requires modelling nonlinear structural behaviour under seismic excitation. Instead, time domain analysis using suites of ground motion records is better suited for SRA within the PBEE framework [5]. In the PBEE framework, the SRA problem is often simplified to determine the probability of failure, where the maximum seismic response surpasses a predefined allowable value during the entire duration of an earthquake. This simplification is carried out to ensure that a specific performance level is achieved for the structure under consideration [6]. Hence, the performance function or limit state function (LSF) can be expressed as,

$$g(\mathbf{X}) = \min_{t}[C(\mathbf{X}_{\mathrm{C}}, t) - D(\mathbf{X}_{\mathrm{D}}, t)] \tag{1}$$

where, g, C and D are the LSF, the capacity and demand functions, respectively; $\mathbf{X}$ consists of two vectors, $\mathbf{X_C}$ and $\mathbf{X_D}$ which respectively represent the resistance and load-related variables and t is the time parameter. The conditional probability of reaching a specific limit state, or in other words, the probability of failure for a given value of an intensity measure, is often referred to as a fragility curve [7]. When failure occurs in a structure, it is generally represented by the condition $g(\mathbf{X}) \leq 0$, and the probability of failure (P_f), can be mathematically expressed as a multi-dimensional integral over the joint probability density function (PDF), $f_{\mathbf{X}}$ of the random variables in $\mathbf{X}$, as,

$$P_f = \iint_{g(\mathbf{X})\leq 0} \cdots \int f_{\mathbf{X}}(\mathbf{X}) d\mathbf{X} \tag{2}$$

The accurate evaluation of the integral mentioned above often requires significant computational resources. Various approximations are commonly used to estimate the probability of exceeding a given threshold value for a limit state of damage in response to seismic actions. Several review articles have covered related developments in seismic performance assessment of structures, encompassing seismic action modelling, seismic response analysis, and fragility assessment [5,8,9]. In this regard, a more precise and conceptually straightforward approach for SRA is based on the Monte Carlo simulation (MCS) technique. It is widely recognised for its validity and robustness [10]. However, the primary hindrance of this approach is that it demands a large number of repetitive nonlinear time history analyses (NLTHA) of the structure under consideration to achieve an acceptable level of confidence in estimating the P_f value, resulting in high computational expenses.

The metamodeling technique has emerged as a promising alternative to address the challenge of computationally intensive repetitive NLTHA. Metamodeling involves constructing surrogate models (metamodels) that approximate the complex and computationally expensive implicit LSF. These metamodels are more straightforward and faster to evaluate than the original model. One can perform probabilistic analyses using metamodels with significantly fewer NLTHA, saving computational resources while still maintaining reasonable accuracy in estimating the P_f values. Among various metamodeling techniques, applying the least squares method (LSM) based polynomial response surface method (RSM) is the simplest and most commonly used metamodeling technique in SRA of structures [6,11–17]. However, it has limitations in predicting nonlinear responses accurately in some local regions of interest, which is otherwise essential for accurately estimating failure probability. The global nature of LSM-based RSM can be a significant source of error, as it may not fully capture the complex variations within specific regions of the input space [18]. Various advanced metamodeling techniques address this limitation by their ability to adaptively approximate the local trend of an LSF. For example, the successful application of moving LSM-based RSM [19], artificial neural networks [20,21], support vector regression [22,23], Kriging [24,25] etc., may be noted. However, applying such metamodeling techniques for SRA is quite challenging due to the high-dimensional nature of earthquake input parameters, leading to several input variables needed to accurately approximate output responses. This difficulty is addressed by a common approach that partitions the input variable space into two groups, i.e. the structural parameters and the stochastic sequences. One approach that utilises such a concept of separation is the SRA by RSM with a random factor [6]. The other commonly used technique is the dual RSM [26], which also typically divides the input space into two vectors to improve the efficiency of the analysis. The latter approach has been widely employed for the SRA of structures [13–17,19,27–30]. However, the dual metamodeling approach in SRA requires prior assumptions about seismic response distributions. An alternative metamodeling approach in SRA is to use techniques like high-dimensional model representation (HDMR) that decomposes the nonlinear input-output relationship to effectively handle high-dimensional input spaces and provide accurate approximations of the relation between seismic responses and uncertain inputs of the structural models [31,32]. In addition to the methods mentioned earlier, earthquake accelerations can be treated as input variables to the metamodel, and the structural response time history is predicted directly [33]. A recent application of such an approach using deep neural networks for SRA is worth noting [34].

The success of a metamodel in the reliability analyses of structures relies profoundly on the selection of training samples during the design of experiments (DOE). Adaptive sampling, which involves increasing the training samples iteratively near the limit state, is a decisive approach widely applied to enhance the accuracy and effectiveness of structural reliability analysis [35–49]. Among these strategies, the active learning-based approach has received significant attention. Active learning-based algorithms, such as those proposed by Echard et al. [37] and Bichon et al. [50], have been widely applied. In this regard, a recent review article on active learning in structural reliability analysis by Moustapha et al. [51] offers a comprehensive overview of this rapidly evolving area. However, implementing adaptive training near the limit state in metamodeling-based SRA is challenging due to the record-to-record variation of earthquakes. For this reason, there are limited studies on the adaptive metamodeling approach for SRA [52–54]. Nonetheless, these adaptive metamodeling approaches rely on the lognormal assumptions of seismic responses. This assumption necessitates the calculation of the mean and standard deviation of seismic responses at each new training point, which results in the evaluation of seismic responses for all ground motion records considered to account for record-to-record variations. As a consequence, the total number of NLTHA and the computation cost increase significantly. This issue needs to be addressed in developing any adaptive metamodeling approach so that the total number of NLTHAs is reduced for an efficient SRA.

The present study aims to develop an active learning-based adaptive metamodeling approach for SRA that does not rely on any prior distribution assumptions about nonlinear seismic responses. For this, separate metamodels are constructed to approximate the responses of each earthquake in the suite of ground motion records, which are built to address the record-to-record variation of earthquakes. This concept was previously studied for SRA using support vector regression [22], and Kriging [25] metamodels, but both studies employed a single-shot DOE for metamodel training. Very recently, the support vector regression-based approach has been further improved by an adaptive training scheme [23]. In the present study, separate metamodels are updated using an active learning algorithm to improve accuracy near the limit state. Unlike existing active learning approaches for SRA, the addition of a new training point incurs only one NLTHA corresponding to the specific ground motion of interest. As a result, the total number of NLTHA runs is anticipated to be significantly reduced. This reduction in NLTHA leads to a more efficient and computationally cost-effective metamodeling approach for SRA. Further, sparse Bayesian regression

is chosen as the metamodeling technique due to its computational efficiency, thanks to the sparsity involved in sparse Bayesian learning. The proposed approach offers improved performance compared to the existing active learning-based adaptive approach in terms of accuracy and computational cost. Two realistic numerical examples of SRA are presented to demonstrate the effectiveness of the proposed approach. These examples showcase how the sparse Bayesian regression-based adaptive metamodeling approach outperforms the existing approach, providing enhanced accuracy while reducing computational expenses. Overall, this research aims to contribute to the field of SRA by introducing a novel metamodeling technique that addresses the challenges associated with accurate nonlinear seismic response approximation by adaptive training avoiding prior distribution assumptions. The article provides a comprehensive explanation of the proposed approach and demonstrates its efficacy through numerical illustrations.

2. Seismic reliability analysis

2.1. Nonlinear time history analysis of structures subjected to seismic excitation

The dynamic response of structural systems to transient loads can be obtained by direct numerical integration of the equations of motion in the time domain. The Newmark-β method, proposed initially by Newmark in 1959 [55], has become one of the most widely used time integration schemes for structural dynamics. The incremental equations of motion for a single-degree-of-freedom structural system subjected to seismic excitation can be expressed as [56]:

$$m_0\Delta\ddot{u} + c_t\Delta\dot{u} + k_t\Delta u = -m_0\Delta\ddot{u}_g \tag{3}$$

Where, m_0 is the mass, c_t and k_t are the initial tangent coefficients of damping and stiffness, respectively at the beginning of the time step. For the considered time interval $\Delta t = t_{i+1} - t_i$, Δu, $\Delta\dot{u}$, $\Delta\ddot{u}$ and $\Delta\ddot{u}_g$ represent the different incremental motions. u, $\dot{u}$ and $\ddot{u}$ are the relative displacement, relative velocity and relative acceleration of the mass with respect to support, respectively, and $\ddot{u}_g$ is the ground motion applied at the support. Using the Newmark-β method, the equation of motion at time t_{i+1} is solved using the known displacement, velocity, and acceleration at time t_i and the excitation at time t_{i+1}. The Newmark-β method basically adopts the following relationships [55,56],

$$\Delta\dot{u} = \Delta t\ddot{u}_i + \delta\Delta t\Delta\ddot{u} \tag{4}$$

$$\Delta u = \Delta t\dot{u}_i + \frac{(\Delta t)^2}{2}\ddot{u}_i + \beta(\Delta t)^2\Delta\ddot{u} \tag{5}$$

where δ and β are free parameters. The commonly used average acceleration method corresponds to $\delta = 1/4$ and $\beta = 1/2$. Rearranging Eq. (5), $\Delta\ddot{u}$ is obtained as:

$$\Delta\ddot{u} = \frac{1}{\beta(\Delta t)^2}\Delta u - \frac{1}{\beta\Delta t}\dot{u}_i - \frac{1}{2\beta}\ddot{u}_i \tag{6}$$

Substituting the value of $\Delta\ddot{u}$ into Eq. (4) gives,

$$\Delta\dot{u} = \frac{\delta}{\beta\Delta t}\Delta u - \frac{\delta}{\beta}\dot{u}_i + \Delta t\left(1 - \frac{\delta}{2\beta}\right)\ddot{u}_i \tag{7}$$

Substituting $\Delta\dot{u}$ and $\Delta\ddot{u}$ into Eq. (3) gives,

$$\bar{k}\Delta u = \Delta p \tag{8}$$

in which

$$\begin{aligned}\bar{k} &= k_t + \frac{\delta}{\beta\Delta t}c_t + \frac{1}{\beta(\Delta t)^2}m_0\\ \Delta p &= -m_0\Delta\ddot{u}_g + \left(\frac{m_0}{\beta\Delta t} + \frac{\delta}{\beta}c_t\right)\dot{u}_i + \left[\frac{m_0}{2\beta} + \Delta t\left(\frac{\delta}{2\beta} - 1\right)c_t\right]\ddot{u}_i\end{aligned} \tag{9}$$

Solution of Eq. (8) provides the incremental displacement, Δu. Finally, the responses at time t_{i+1} are obtained as,

$$u_{i+1} = u_i + \Delta u; \quad \dot{u}_{i+1} = \dot{u}_i + \Delta\dot{u}; \quad \ddot{u}_{i+1} = \ddot{u}_i + \Delta\ddot{u} \tag{10}$$

The formulation for a single-degree-of-freedom system presented above can be easily expanded to multi-degree-of-freedom structural systems [56]. The outlined solution method remains valid if damping and restoring force nonlinearities follow identical load-unload paths. The solution procedure is the same for geometrically nonlinear problems with linear damping. However, with material nonlinearity and linear damping, as typical under seismic loading, the solution must account for hysteretic force-deformation behaviour. In such cases, the procedure requires modification to minimise unbalanced forces when stiffness varies during time stepping. Specifically, an iterative approach is needed to track varying stiffness from loading reversals and satisfy dynamic equilibrium.

For instance, in the modified solution procedure for elastoplastic material [56], the damping coefficient c_t is taken as constant; the stiffness k_t varies between the initial elastic stiffness k_0 and zero based on the deformation state. Specifically, k_t equals the initial k_0 during elastic loading and unloading when the response follows the initial stiffness path. In contrast, k_t becomes zero during plastic deformation when the system exhibits no additional stiffness. Tracking k_t based on the current elastic or plastic condition enables the proper capture of hysteretic behaviour. The solution procedure checks elastic versus plastic deformation states at the beginning and end of each time step. For steps that remain entirely elastic, the computations normally proceed to the next increment. However, if yielding occurs within a step, indicated by the transition from elastic to plastic, the calculations are restarted for that specific increment. This involves first computing an elastic displacement increment $(\Delta u)_e$ as a fraction of the calculated initially total increment $(\Delta u)_0$:

$$(\Delta u)_e = a_e(\Delta u)_0 \tag{11}$$

where a_e is a scalar (less than 1) such that the system just reaches yielding. After computing the elastic sub-increment, the plastic displacement $(\Delta u)_p$ is calculated by applying the remaining load fraction $(1 - a_e)\Delta p$ using Eq. (8). This plastic increment evaluation sets stiffness $k_t = 0$, representing zero stiffness in the post-yield regime. Finally, the total displacement for the entire time step equals the sum of the elastic displacement fraction $(\Delta u)_e$ and plastic displacement increment $(\Delta u)_p$. After initial plastic yielding, the system remains plastic while velocity stays positive, indicating continued displacement increase. The solution continues using Eq. (8) with $k_t = 0$ during this plastic deformation phase. Once velocity becomes negative, signifying unloading, the state switches from plastic back to elastic within the same time step. For this elastic unloading, the computations are restarted with elastic stiffness k_t restored. The solution must detect when velocity becomes zero during unloading, indicating the reversal point. This is done by factoring the originally calculated displacement increment Δu by a scalar e to make the total displacement $u(t)$ have zero velocity $\dot{u}(t) = 0$. The load decrement $(1 - e)\Delta p$ then gives the remaining unloading increment $(\Delta u)_a$ using Eq. (4) with restored elastic stiffness k_t. Finally, the total step displacement Δu is the sum of $e\Delta u$ and $(\Delta u)_a$.

2.2. Metamodel-based seismic reliability analysis of structures

Unlike reliability analyses of structures under static or deterministic dynamic loads, applying the metamodeling approach for SRA poses significant challenges. The primary difficulty arises from dealing with a large number of input parameters due to the high-dimensional nature of earthquake input forces. To address this issue, the dual RSM has been commonly employed [26]. Instead of modelling the seismic excitation as a random input parameter, the analysis involves considering a set of ground motions to implicitly incorporate the impact of record-to-record

variations in the assessment. In the dual metamodeling approach, the mean and standard deviation of the desired seismic responses for all ground motions in the suite are approximated by two separate metamodels. It is assumed that the overall seismic response follows a certain distribution (mostly lognormal) with the obtained mean and standard deviation. By utilising the approximated overall seismic response, the failure probability for a given seismic intensity level can be calculated through the MCS technique. On the other hand, separate metamodels can be constructed to approximate the responses of each ground motion, and the approximated response corresponding to a randomly selected ground motion is used by the MCS technique to estimate failure probability at a given seismic intensity level [22,25]. The latter approach does not rely on any prior distribution assumption as required in the dual metamodeling approach. Like the direct MCS technique, one ground motion is randomly selected from the suite and each record has an equal probability of being chosen. If m ground motions are considered in the suite, then $\widehat{y}_k(\mathbf{x})$ for $k = 1, 2, \ldots, m$ i.e., m metamodels for each of them are constructed as a function of uncertain structural parameters $\mathbf{x}$. Once the metamodels are built for all the ground motions in the bin, the MCS technique is readily performed for SRA by generating random samples of input parameters $\mathbf{x}$ based on the associated PDFs and random selection of metamodel from the bin. Such random selection of metamodel from the bin implicitly incorporates the conventional notion of considering record-to-record variations of earthquake motion. This is based on the assumption that the ground motions in the bin obtained for a target hazard level have an equal probability of occurrence i.e. any earthquake of specific intensity is equally likely to occur. Therefore, the present approach needs sample generation for input parameters $\mathbf{x}$ only. Additionally, the metamodel incorporates the earthquake intensity parameter as an extra dimension, alongside the structural uncertain parameters, to estimate the seismic reliability effectively at various intensity levels [27]. In the present study, the peak ground acceleration (PGA) is chosen as the intensity measure and $\widehat{y}_k(\mathbf{x})$ is modified by including its dependency on PGA as $\widehat{y}_k(\mathbf{x},\mathrm{PGA})$. However, the approach is generic, and any other seismic intensity measure can be used.

3. Proposed adaptive sparse Bayesian regression for seismic reliability analysis of structures

The present study relies on the sparse Bayesian regression-based metamodeling approach for the SRA of structures. Thus, before developing the proposed adaptive approach, the mathematical formulations of sparse Bayesian regression are briefly presented for a smooth transition.

3.1. Sparse Bayesian regression

Sparse Bayesian regression is a probabilistic framework for learning in models expressed as a linearly weighted sum of basis functions, where the output is a function of the input space. In contrast to conventional regression techniques, where point estimates are only computed for the regression coefficients (i.e., weight parameters), a Bayesian regression estimates distributions over the parameters and predictions. The sparse Bayesian learning process involves inferring the parameters of the regression function from a training dataset. It combines the advantages of Bayesian inference with sparsity-inducing techniques, allowing for the automatic selection of essential basis functions while estimating their associated weight coefficients. In sparse Bayesian regression, most of the weight parameters are automatically set to zero during the learning process, making the predictor sparse as it contains very few non-zero coefficients relevant to making good predictions [57]. This effectively circumvents the overfitting, i.e. a generalisation ability of the prediction. The key feature of this approach is that apart from offering a good generalisation performance, the inferred predictors are exceedingly sparse in that they contain relatively few non-zero regressor parameters. Whereas the traditional Bayesian regression makes predictions using all possible regression weights, weighted by their posterior probability. The solution has no sparsity, as all regression coefficients have non-zero values. Consequently, the traditional Bayesian regression does not have a good generalisation performance like sparse Bayesian regression. The model is mathematically represented as:

$$y(\mathbf{x};\mathbf{w}) = \sum_{m=1}^{M} \omega_m \varphi_m(\mathbf{x}), \tag{12}$$

where, $y(\mathbf{x})$ is the predicted output value for input $\mathbf{x}$, M is the number of basis functions used, $\varphi_m(\mathbf{x})$ represents these basis functions (which can be nonlinear and predefined), and $\mathbf{w} = \{\omega_1, \omega_2, \ldots, \omega_M\}^{\mathrm{T}}$ is the parameter vector where ω_m are adjustable parameters (also known as weights) associated with each basis function. The appropriate values for the weights that best fit the training data are achieved through a Bayesian probabilistic framework for learning, as detailed by Tipping [57].

In this Bayesian learning approach, the target values $\mathbf{t} = \{t_1, t_2, \ldots, t_P\}^{\mathrm{T}}$ in the training dataset $\{\mathbf{x}_i, t_i\}_{i=1}^{P}$ are assumed to be generated from the model $\mathbf{y} = \{y(\mathbf{x}_1), y(\mathbf{x}_2), \ldots, y(\mathbf{x}_P)\}^{\mathrm{T}}$ with additive noise $\boldsymbol{\varepsilon} = \{\varepsilon_1, \varepsilon_2, \ldots, \varepsilon_P\}^{\mathrm{T}}$ i.e.,

$$\mathbf{t} = \mathbf{y} + \boldsymbol{\varepsilon} = \boldsymbol{\Phi}\mathbf{w} + \boldsymbol{\varepsilon} \tag{13}$$

Where, $\boldsymbol{\Phi}$ represents the $P \times M$ design matrix where each row corresponds to a training data point, and the row itself contains the M basis functions for that data point. It is further assumed that $\boldsymbol{\varepsilon}$ contains independent samples from a Gaussian process with zero mean and variance σ^2, i.e., $p(\boldsymbol{\varepsilon}) = \prod_{i=i}^{P} \mathcal{N}(\varepsilon_i|0,\sigma^2)$. Consequently, the error model leads to a multivariate Gaussian likelihood for the complete dataset, given by,

$$p(\mathbf{t}|\mathbf{w},\sigma^2) = (2\pi)^{-P/2}\sigma^{-P}\exp\left(-\frac{\|\mathbf{t}-\boldsymbol{\Phi}\mathbf{w}\|^2}{2\sigma^2}\right). \tag{14}$$

However, when performing maximum likelihood estimation of $\mathbf{w}$ and σ^2 with as many parameters in the model as training examples, it can lead to severe overfitting. To prevent overfitting, a Gaussian prior distribution is defined over $\mathbf{w}$, with a vector of independent hyperparameters $\boldsymbol{\alpha} = \{\alpha_1, \alpha_2, \ldots, \alpha_M\}^{\mathrm{T}}$ controlling the relevance of each parameter, as follows,

$$p(\mathbf{w}|\boldsymbol{\alpha}) = \prod_{m=1}^{M} \mathcal{N}(\omega_m|0,\alpha_m^{-1}) = (2\pi)^{-M/2}\prod_{m=1}^{M}\alpha_m^{1/2}\exp\left(-\frac{\alpha_m\omega_m^2}{2}\right). \tag{15}$$

As a type of automatic relevance determination prior, this encourages sparsity, meaning some parameters may be set to zero, leading to a simpler model with fewer basis functions [57]. The posterior distribution of the parameter vector $\mathbf{w}$ given the data is obtained by combining the likelihood (Gaussian noise model) with the prior using Bayes' rule as follows,

$$p(\mathbf{w}|\mathbf{t},\boldsymbol{\alpha},\sigma^2) = \frac{p(\mathbf{t}|\mathbf{w},\sigma^2)p(\mathbf{w}|\boldsymbol{\alpha})}{p(\mathbf{t}|\boldsymbol{\alpha},\sigma^2)}. \tag{16}$$

The resulting posterior is a Gaussian distribution with updated mean $\boldsymbol{\mu}$ and covariance $\sum$, which can be expressed as,

$$\boldsymbol{\mu} = \sigma^{-2}\sum\boldsymbol{\Phi}^{\mathrm{T}}\mathbf{t}\sum = \left(\mathbf{A}+\sigma^{-2}\boldsymbol{\Phi}^{\mathrm{T}}\boldsymbol{\Phi}\right)^{-1}, \tag{17}$$

Where, $\mathbf{A}$ defined as diag($\boldsymbol{\alpha}$), i.e., diagonal matrix with vector $\boldsymbol{\alpha}$. Bayesian inference over the hyperparameters is theoretically challenging, so a most-probable point estimate $\boldsymbol{\alpha}_{MP}$ is typically obtained using a type-II maximum likelihood procedure [58]. Sparse Bayesian learning is achieved by maximising the marginal likelihood (or its logarithm) with respect to the hyperparameters $\boldsymbol{\alpha}$, as follows,

Table 1
Comparison of computational time for predicting response for varying input dimensions and training data size.

Sparse Bayesian regression (Kriging)	Time Required (in seconds)			
	For 3 input variables	For 5 input variables	For 8 input variables	For 10 input variables
50 training data	1.70 (4.05)	1.80 (4.72)	2.12 (5.72)	2.16 (6.64)
250 training data	1.70 (30.6)	1.80 (35.1)	2.16 (37.5)	2.63 (40.8)
500 training data	1.70 (101)	1.80 (108)	2.18 (116)	2.64 (121)
750 training data	1.70 (212)	1.80 (222)	2.19 (243)	2.67 (248)
1000 training data	1.70 (422)	1.80 (433)	2.28 (452)	2.70 (467)

$$\mathscr{L}(\boldsymbol{\alpha}) = \log p\left(\mathbf{t}|\boldsymbol{\alpha},\sigma^2\right) = \log \int_{-\infty}^{\infty} p\left(\mathbf{t}|\mathbf{w},\sigma^2\right) p(\mathbf{w}|\boldsymbol{\alpha}) d\mathbf{w} = -\frac{1}{2}\left[N\log 2\,\pi + \log|\mathbf{C}| + \mathbf{t}^{\mathrm{T}}\mathbf{C}^{-1}\mathbf{t}\right] \tag{18}$$

Where, $C = \sigma^2\mathbf{I} + \boldsymbol{\Phi}\mathbf{A}^{-1}\boldsymbol{\Phi}^{\mathrm{T}}$. Once the hyperparameters are estimated, prediction y_* and its variance σ_*^2 can be made by evaluating the model at a new point $\mathbf{x}_*$ using the learned parameters and the basis functions as,

$$y_* = \boldsymbol{\varphi}(\mathbf{x}_*)\boldsymbol{\mu}_{MP} \tag{19}$$

$$\sigma_*^2 = \sigma_{MP}^2 + \boldsymbol{\varphi}(\mathbf{x}_*)\sum\nolimits_{MP}\boldsymbol{\varphi}(\mathbf{x}_*)^{\mathrm{T}} \tag{20}$$

Where, $\boldsymbol{\varphi}(\mathbf{x}_*)$ represents the row vector of the basis functions at $\mathbf{x}_*$; $\sum_{MP}$ and $\boldsymbol{\mu}_{MP}$ are obtained by substituting $\boldsymbol{\alpha} = \boldsymbol{\alpha}_{MP}$ and $\sigma^2 = \sigma_{MP}^2$ in Eq. (17).

The basis functions are broadly categorised into two types, namely, fixed and data-centred. The fixed basis can be linear, nonlinear, or higher-order polynomials. The data-centred basis functions are generally made of kernel functions involving prerequisite kernel parameter (s). The data wastage and additional computational time for proper selection of such parameter(s) are the main disadvantages of using data-centred basis functions. In contrast, a fixed basis is free from such disadvantages. The performances of using two fixed-type basis functions, namely, the first- and second-order polynomial functions, for the active learning-enhanced sparse Bayesian regression to estimate reliability are demonstrated by Roy et al. [48]. The superior performance of the second-order polynomial basis function was observed. Following this, the second-order polynomial is chosen as the basis function in the present study. In such a polynomial with n variables, a total of $\frac{(n+1)(n+2)}{2}$ basis functions can be expressed as, $(\mathbf{x}) = \left[1, x_1, \cdots, x_n, x_1^2, x_1x_2, \cdots, x_{n-1}x_n, x_n^2\right]$.

The computational involvement of the proposed sparse Bayesian regression and the most commonly used Kriging model are studied by comparing the computational time for constructing a metamodel and approximating the LSF at one million points by the metamodel for different input dimensions and training data sizes in Table 1. The time required by the Kriging approach is shown in brackets. The computation time shown excludes the generation of training data. Thus, this comparison is independent of the nature of the numerical example except the input dimension. The computation time slightly increases with respect to the input dimension, and changes are insignificant with regard to training data size in the case of sparse Bayesian regression. The computation time for Kriging increases significantly with both input dimension and training data size.

3.2. Proposed active learning-based adaptive metamodeling approach of seismic reliability analysis

The proposed adaptive metamodeling approach differs from the dual metamodeling approach in its fundamental requirement. The approach no longer necessitates any prior distribution assumptions for seismic responses. Instead of constructing metamodels solely for the mean and standard deviation of seismic responses, the new approach adopts a more refined strategy. Separate metamodels are built to approximate the seismic response for each ground motion within the specified suite. Without prior information about the failure plane, treating the entire input space as equally important when selecting initial training points becomes necessary. To achieve this, a space-filling design, i.e. uniform design (UD) is employed. This design ensures the lowest discrepancy from a uniform distribution [59], allowing for the construction of an initial DOE that effectively covers the input space. The initial DOE is common for all distinct initial metamodels, each corresponding to different ground motions in the suite. However, the failure plane corresponding to a particular ground motion exhibits a shift for changes in PGA levels and varies significantly across different damage states. As a result, it becomes necessary to implement separate adaptive sampling processes for each PGA level and damage state. The present approach accurately represents the complex relationships between ground motion, PGA levels, damage states, and the corresponding failure planes.

The values of P_f at various PGA levels are required to obtain for seismic vulnerability assessment of structures. An MCS population of N_{MC} points consisting of randomly generated samples of the structural parameters is considered to obtain P_f values. The control variable PGA is kept constant for which P_f needs to be calculated. Then, each of the N_{MC} points is randomly assigned to a ground motion from the suite of m number of records. Without loss of generality, it is assumed that N_k points are assigned to k-th ground motion. As mentioned above, the proposed approach updates the metamodel for any ground motion at each of all possible combinations of damage state and PGA level. The U function developed by Echard et al. [37] is employed as the learning function for selecting new sample points by the proposed active learning algorithm. If a metamodel has the LSF prediction $\widehat{\mu}(\mathbf{x})$ and its predictive variance $\widehat{\sigma}(\mathbf{x})$ at a point $\mathbf{x}$, then the U function can be evaluated as $U(\mathbf{x}) = \frac{|\widehat{\mu}(\mathbf{x})|}{\widehat{\sigma}(\mathbf{x})}$ at that point. Interestingly, the standard normal cumulative density function (CDF) of the negative of this learning function represents the probability of a point being misclassified, i.e., having a wrong sign assignment for the LSF. Following this, the stopping criterion for the U function is set to $U > 2$, which corresponds to a probability of less than 0.023 for such a mistake, as originally recommended by Echard et al. [37]. On the other hand, a stopping criterion based on the stabilisation of the failure estimate has recently been endorsed by Roy et al. [48] for the U function-based active learning algorithm, where sparse Bayesian regression is used as the metamodeling technique. The stabilisation is deemed achieved when ten consecutive iterations produce failure estimates within ±1% of the latest estimate. In the present study, both stopping criteria are applied simultaneously to prevent unnecessary wastage of data. The step-by-step procedure of the proposed active learning-based adaptive metamodeling approach for k-th ground motion at a specific value of PGA is presented below.

Step 1 - Select an initial DOE with p_0 training samples following a UD over the entire input space.
Step 2 - Based on the DOE, train the metamodel.
Step 3 - Evaluate the LSF prediction and its variance at the N_k points from the latest metamodel.
Step 4 - Estimate the number of failure points ($\widehat{n}_f^k$) among the N_k points.
Step 5 - If the $\widehat{n}_f^k$ in the previous 10 iterations is within ±1% of the present $\widehat{n}_f^k$ then updating of the metamodel is stopped and go to step 9.
Step 6 - Calculate the values of the U function at the N_k points.
Step 7 - If the minimum value of the U function is greater than 2, go to step 9. (i.e., no new training point will be added)
Step 8 - Select the point corresponding to the minimum value of the U function. Add it as a new training sample into the DOE and go to step 2.

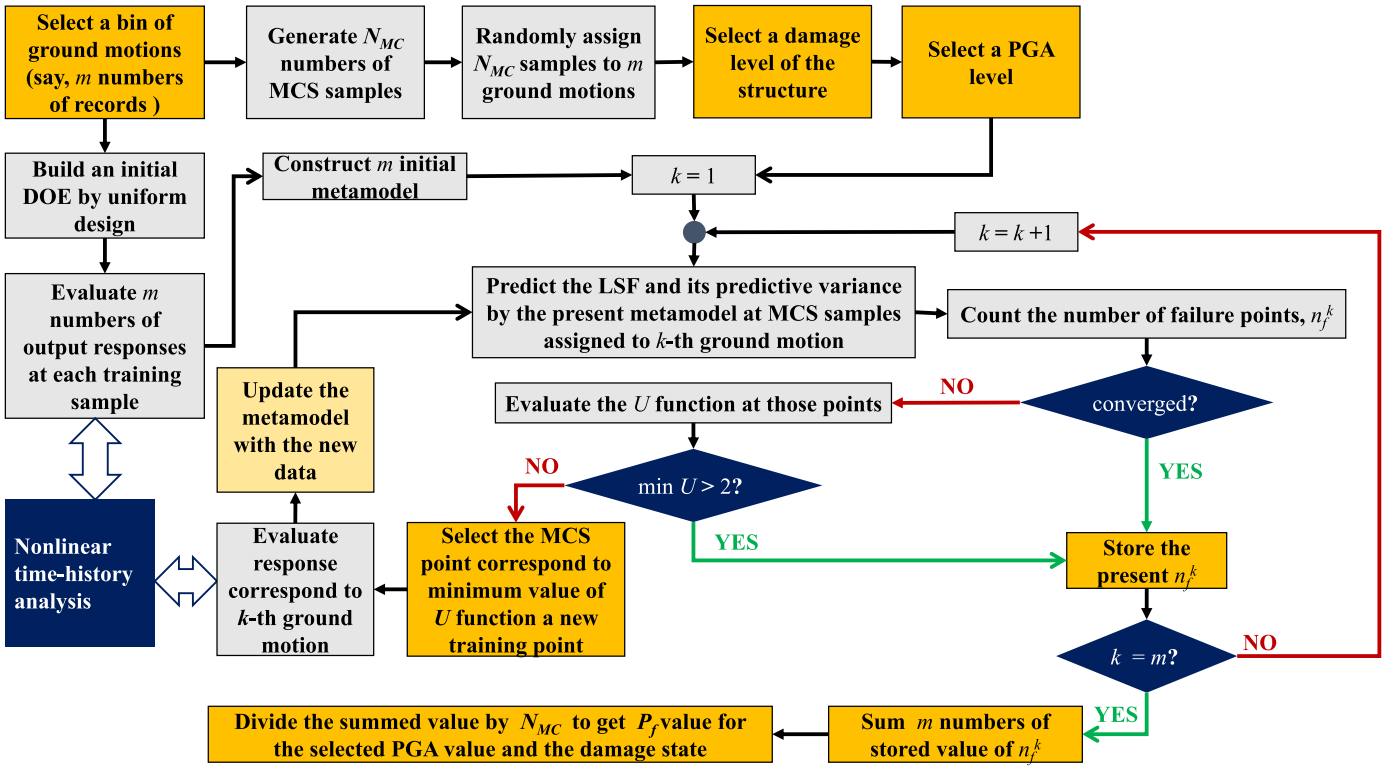

Fig. 1. Flowchart of the proposed active learning-based adaptive metamodeling approach for SRA.

Step 9 - The latest value of the number of failure points is considered as the converged result $\hat{n}^k_{f,converged}$.

In this way, starting from a common initial DOE, m numbers of adaptive metamodels for m number of ground motion records are updated until the convergence. The P_f value at the desired value of PGA is finally estimated in the MCS framework as,

$$\hat{P}_{f,PGA} = \frac{\sum_{k=1}^{m} \hat{n}^k_{f,converged}}{\sum_{k=1}^{m} N_k} = \frac{\sum_{k=1}^{m} \hat{n}^k_{f,converged}}{N_{MC}} \tag{21}$$

A flowchart of the proposed active learning-based adaptive metamodeling approach is depicted in Fig. 1.

For any other value of PGA, the iterations start from the same initial

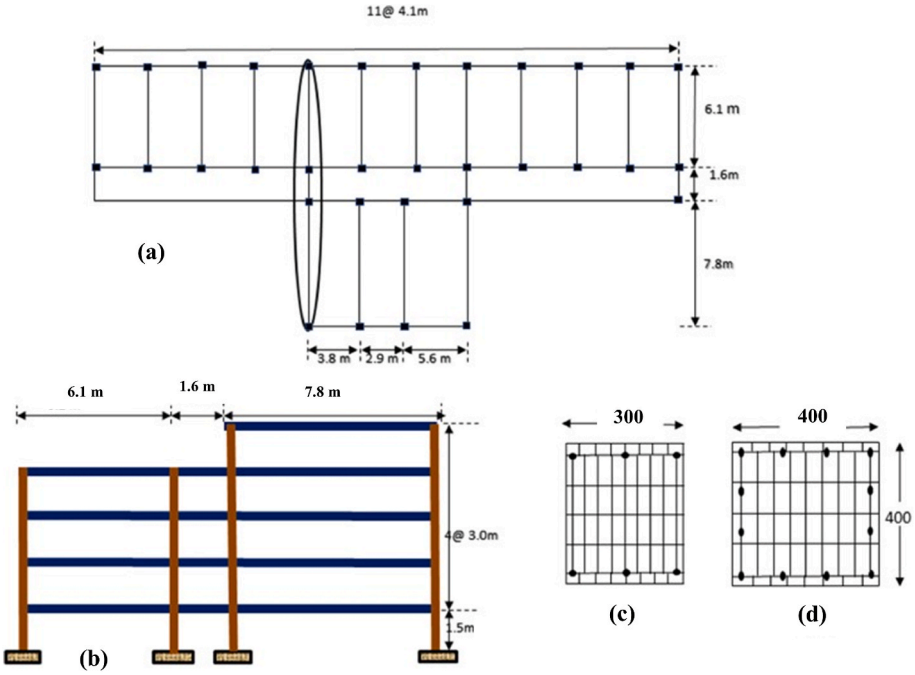

Fig. 2. (a) The building plan, (b) the details of the extracted 2D frame, (c) the details of the fibre discretisation of the beams and (c) the columns [22].

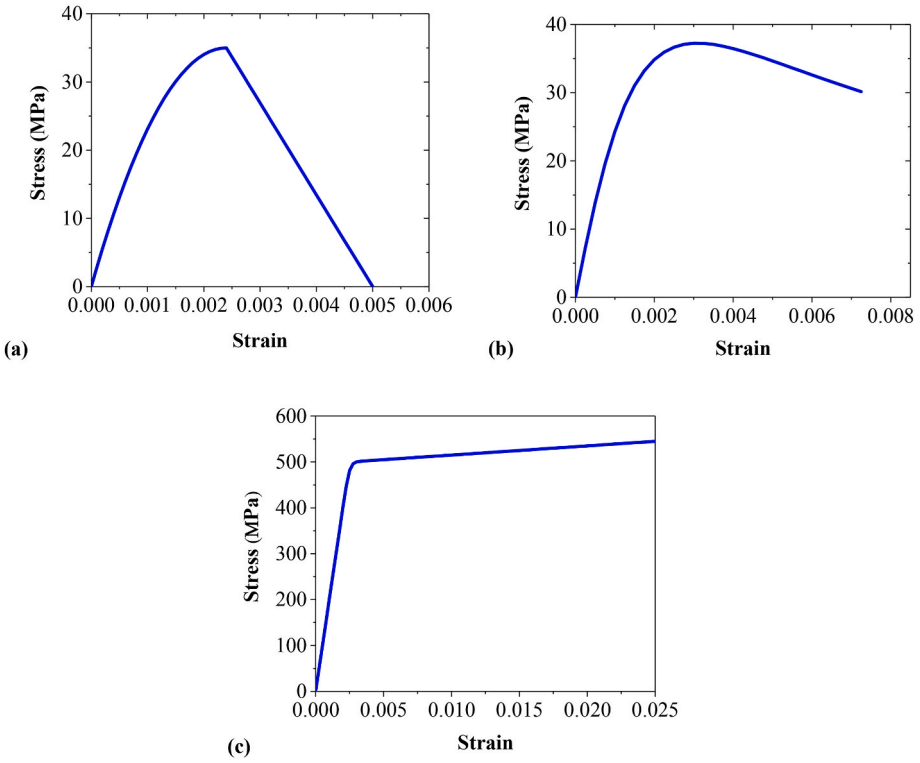

Fig. 3. The stress-strain behaviour of (a) unconfined cover concrete as per the concrete01 model, (b) confined core concrete as per the concrete04 model for 28-days compressive strength of 35 MPa and (c) reinforcing steel as per the steel02 model for yield strength of 500 MPa.

DOE. However, the adaptive samples vary depending on the PGA value and the considered ground motion. In the case of multiple damage levels, the initial DOE remains identical for all LSFs, but the adaptive samples are different. As a result, different new training points are added, leading to the construction of separate adaptive metamodels.

4. Numerical study

To numerically validate the proposed sparse Bayesian regression-based adaptive metamodeling approach, two realistic examples of SRA of structures are considered. The first example involves the SRA of a typical reinforced concrete (RC) frame of a four-story hostel building. The second example focuses on the SRA of a typical pier in a multi-span river bridge. Both examples require NLTHA to evaluate the seismic response. For the comparative study, the active learning-based adaptive metamodeling approach for SRA, recently developed by Xiao et al. [52], is also employed in combination with the Kriging metamodeling technique as this metamodel is commonly used in active learning algorithms. All figures and tables label this approach as 'Active Kriging'. For both SRA problems, $N_{MC} = 5000$ samples are generated to conduct MCS. The results obtained from the direct MCS technique are considered to be the benchmark for comparison.

4.1. Example 1: A four-storied RC building frame

A four-storied RC building frame problem previously studied by Ghosh et al. [22] is taken as the first example. In the study conducted by Ghosh et al. [22], the 13.5 m high building was considered to be located in Guwahati, India. Accordingly, the ground motion suite consists of twenty-four earthquake time histories for that location, encompassing natural, artificial, and synthetic records, with eight in each category [22]. Eight natural earthquake accelerogram records were chosen from past regional events to match the seismic hazard at the building site. The selection includes earthquakes with magnitude 6.0 to 8.0 within 300 km of the site, covering the magnitude-distance distribution from the disaggregation of the probabilistic seismic hazard analysis [28]. All records are for rock sites, consistent with the site conditions at the building location. Artificial accelerograms were generated to match the target response spectra for rock and stiff soil sites at 5% damping. The simulated accelerograms were modulated using a deterministic envelope function to capture the nonstationary, transient nature of actual earthquakes [28,60]. The stochastic ground motion simulation method proposed by Boore [61] was utilised to develop synthetic accelerations covering magnitude 6.0 to 8.0 events within a 300 km distance. The plan of the entire building and the position of the transverse frame used for SRA are shown in Fig. 2. The cross-sections of beams and columns are 0.3 m × 0.6 m and 0.4 m × 0.4 m, respectively. Steel bars of 16 mm diameter are used for longitudinal reinforcements, with 3 bars placed at the top and bottom of beams and 12 bars equally distributed on the four sides of columns. The stirrups in the beams and lateral ties in the columns are placed at an interval of 0.2 m, utilising reinforcement bars with a diameter of 8 mm. For a more comprehensive understanding of the structural elements, the illustrated fibre discretisation of beams and columns can be found in Ghosh et al. [22].

The NLTHA of the frame is carried out using the OpenSees software [62]. The beams and columns in the model are simulated using displacement-based beam-column elements that incorporate associated fibre sections, with each segment of the beam-column element assigned five integration points to effectively capture the response of the components. In the model, the core sections are represented using confined concrete, while the cover sections are modelled with unconfined concrete. The following material models from the OpenSees are utilised to simulate the nonlinear behaviour of these materials accurately:

i) The concrete04 material model based on Mander et al. [63] is employed for the core concrete, considering its ultimate strength at the stress level corresponding to the first hoop fracture.
ii) The concrete01 material model based on the Kent–Scott–Park concrete material model [64] is used for the cover concrete, which assumes zero tensile strength.

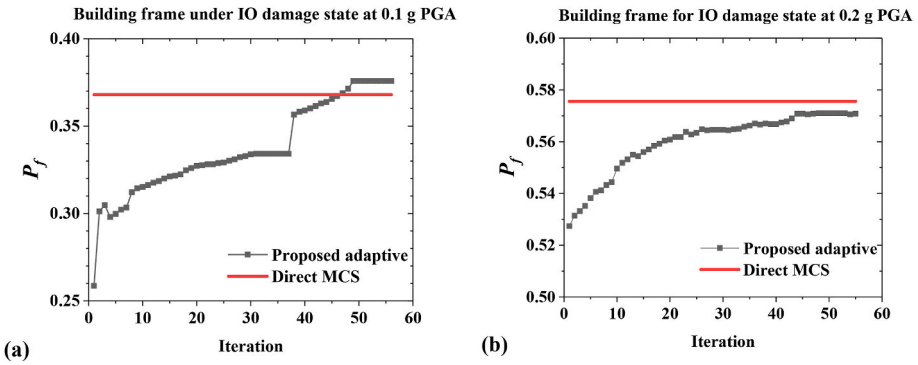

Fig. 4. Convergence of estimated reliability of building frame for IO damage state (a) at 0.1 g PGA level and (b) at 0.2 g PGA level.

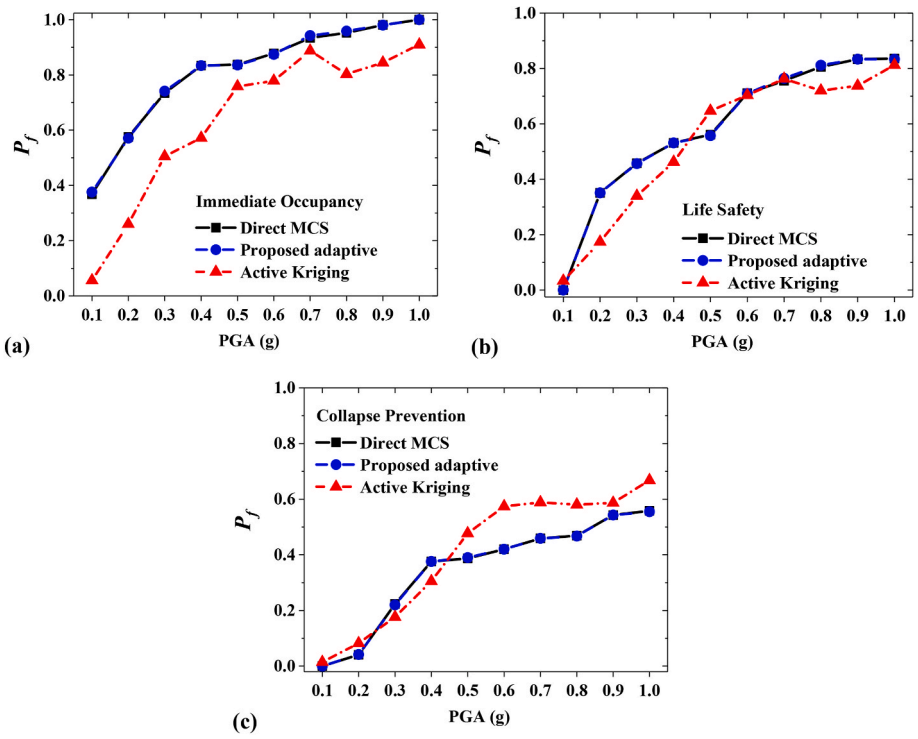

Fig. 5. Seismic reliability of the building frame by different approaches for (a) Immediate Occupancy, (b) Life Safety and (c) Collapse Prevention.

iii) The steel02 material model, which exhibits isotropic strain hardening properties following the Giuffre–Menegotto–Pinto steel material model [65], is selected for the reinforcing steels.

The stress-strain behaviours of the above material models are depicted in Fig. 3.

In the NLTHA, the dead load primarily comprises the self-weight of both the structural and non-structural components. Additionally, a live load of 2 kN/m^2 is assumed for the evaluation. SRA is performed for three structural performance levels: Immediate Occupancy (IO), Life Safety (LS), and Collapse Prevention (CP). The FEMA-356 [66] guidelines provide permissible maximum storey drift ratio values of 1% for IO, 2% for LS, and 4% for CP levels, ensuring structural safety and integrity under varying seismic conditions. In the SRA, the concrete characteristic strength (f_{ck}), steel yield strength (f_y), and structural damping values (ξ) are treated as random variables. They are assumed to follow uncorrelated truncated normal distributions. The mean and standard deviation of f_{ck}, f_y and ξ are taken as 25 MPa and 5 MPa, 250 MPa and 50 MPa, and 5% and 2%, respectively. For truncation of distributions, the considered lower and upper limits of f_{ck}, f_y and ξ are 20 MPa and 30 MPa, 200 MPa and 300 MPa, and 3% and 7%, respectively. In addition to three random variables, PGA is considered the fourth input variable, ranging from 0.1 g to 1.0 g. Based on the UD table $U_{30}(30^4)$ available at https://www.math.hkbu.edu.hk/UniformDesign/, 30 equidistant levels of each variable are arranged to create the initial DOE of 30 training points. After that, the responses of 24 ground motions are evaluated at each of the 30 points, resulting in evaluations of 24 NLTHA for each training point.

The seismic reliability of the building frame under consideration is assessed using the proposed active learning-based adaptive sparse Bayesian regression, the active Kriging and the direct MCS approaches. In the proposed adaptive method, separate adaptive metamodels are built for all 24 ground motions in the bin to approximate the responses for each ground motion under each damage state. Now, adaptive metamodel for each ground motion may require different numbers of adaptive samples. For example, in the case of IO performance level, the adaptive samples needed for each metamodel are varied from 0 to 90. The required number of total adaptive samples is 242 for the IO case. Similarly, the total adaptive samples required are 117 and 0 for the LS and the CP damage cases, respectively. Thus, the proposed adaptive

Table 2
Comparison of the required number of actual function evaluations for SRA of the building frame by different approaches.

PGA	Number of actual function evaluations involving NLTHA	
	Proposed adaptive approach	Active Kriging approach
0.1 g	720 + 359	720 + 1128
0.2 g	720 + 491	720 + 1128
0.3 g	720 + 664	720 + 1080
0.4 g	720 + 173	720 + 840
0.5 g	720 + 423	720 + 984
0.6 g	720 + 305	720 + 888
0.7 g	720 + 185	720 + 1200
0.8 g	720 + 292	720 + 1128
0.9 g	720 + 79	720 + 1200
1.0 g	720 + 114	720 + 1128
Total	720 + 3085	720 + 10704

method requires a total of 359 new training samples for the SRA of the building frame at 0.1g PGA level. Whereas the active learning-based adaptive Kriging method requires 77 adaptive samples for SRA of the building frame at 0.1g PGA. However, one training data generation requires 24 function evaluations involving NLTHAs. Thus, it requires $77 \times 24 = 1128$ NLTHAs of the structure. In the proposed adaptive method, the failure probability gradually becomes more accurate with the increasing number of training points. The gradual changes in failure probability for two typical cases are shown in Fig. 4. Fig. 5 illustrates the seismic reliability of the building frame for three different damage states (i.e., IO, LS, and CP). It is evident from the figure that the results obtained from the proposed approach closely align with those obtained from direct MCS for all cases. However, the active Kriging approach, which relies on the assumption of a lognormal distribution, produces results that significantly deviate from the reference values.

Furthermore, Table 2 compares computational efficiency, i.e. the number of NLTHAs for the different approaches. This comparison provides insights into the efficiency of the approaches in assessing the seismic reliability of the building frame. The total number of adaptive samples added by the proposed approach (3085) is remarkably less than that by the active Kriging approach (10704). Consequently, the total computation time of the proposed approach (20926 s) is also significantly lower than that of the active Kriging approach (41550 s) for the complete generation of seismic reliability results for ten intensity levels.

4.2. Example 2. A typical bridge pier

The second example is a typical bridge pier of a multi-span simply supported river bridge previously investigated by Ghosh et al. [28]. Similar to the previous problem, the bridge is assumed to be located in Guwahati City, and the same ground motion suite is considered for SRA. The longitudinal profile of the bridge, including details about the bent columns, supporting bent cap and pile caps, and their OpenSees model, are shown in Fig. 6. The further details about the OpenSees model of the pier, the displacement-based beam-column elements with associated fibre sections for associated concrete (cover and core separately), modelling of reinforcement and pile resistance including soil-structure interaction effects can be found in Ghosh et al. [28]. Four damage states are considered for SRA. The permissible drift ratios associated with slight, moderate, extensive and complete damage states are taken as 0.01, 0.025, 0.05 and 0.075, respectively [67]. The random variables considered for SRA are the characteristic compressive strength of concrete (f_{ck}), the elastic modulus of concrete (E_c), the yield strength of steel (f_y), the elastic modulus of steel (E_s), translational spring constants ($K_{G,h}$), rotational spring constants ($K_{G,r}$) and the structural damping (ξ). All random variables are considered to be uncorrelated; f_{ck}, f_y and ξ follow truncated normal distributions, while E_c and E_s are distributed as truncated lognormal. The mean and standard deviation of f_{ck}, E_c, f_y, E_s and ξ are taken as 35 MPa and 2.24 MPa, 29580 MPa and 2277.66 MPa, 500 MPa and 32 MPa, 200 GPa and 16 GPa, and 4.5% and 1.25%, respectively. For truncation of distributions, the considered lower and upper limits of f_{ck}, E_c, f_y, E_s and ξ are 32.76 MPa and 37.24 MPa, 27302.34 MPa and 31857.66 MPa, 468 MPa and 532 MPa, 184 GPa and 216 GPa, and 3.25% and 5.75%, respectively. Both $K_{G,h}$ and $K_{G,r}$ are treated as uniform random variables. $K_{G,h}$ varies uniformly between 65.25 kN/mm and 195.75 kN/mm. $K_{G,r}$ ranges uniformly between 3.03×10^5 kN-m/rad and 9.09×10^5 kN-m/rad. There are eight input variables including

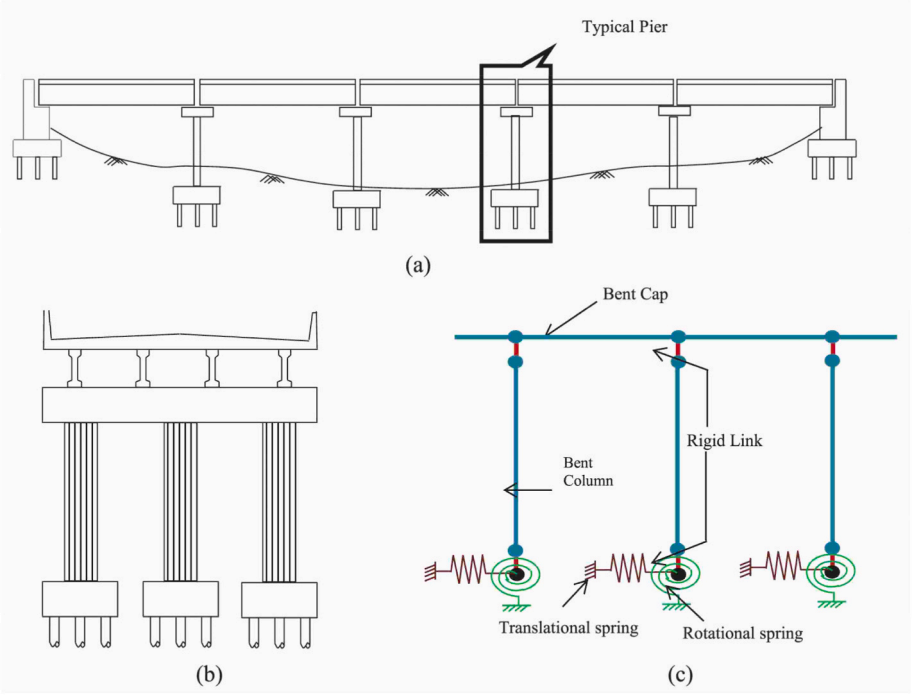

Fig. 6. The details of the considered bridge: (a) longitudinal profile, (b) elevation of the considered multi-column bent, (c) OpenSees analytical model of the bent [22].

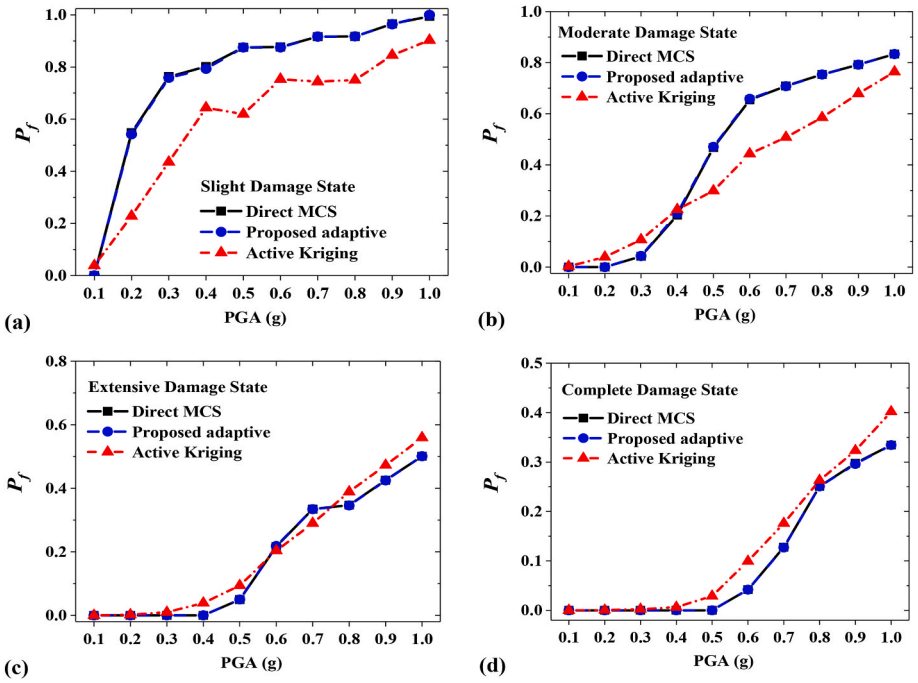

Fig. 7. Seismic reliability of the bridge pier by different approaches for (a) Slight, (b) Moderate, (c) Extensive and (d) Complete damage states.

Table 3
Comparison of the required number of actual function evaluations for SRA of the bridge pier by different approaches.

PGA	Number of actual function evaluations involving NLTHA	
	Proposed adaptive approach	Active Kriging approach
0.1 g	720 + 510	720 + 3408
0.2 g	720 + 652	720 + 3504
0.3 g	720 + 212	720 + 3552
0.4 g	720 + 625	720 + 3624
0.5 g	720 + 385	720 + 3816
0.6 g	720 + 286	720 + 4080
0.7 g	720 + 234	720 + 4272
0.8 g	720 + 430	720 + 3864
0.9 g	720 + 631	720 + 3696
1.0 g	720 + 35	720 + 3264
Total	720 + 4000	720 + 37080

PGA. Therefore, the UD table $U_{30}(30^8)$ generates the 30 initial training points. Subsequently, the responses are evaluated at each training point, resulting in 24 × 30 NLTHA evaluations.

Like the previous problem, the SRA of the bridge pier is performed using the proposed adaptive approach, the active Kriging approach, and the direct MCS approach. Fig. 7 illustrates the seismic reliability of the bridge pier estimated by three approaches for four different damage states. It is evident from the figure that the results obtained from the proposed approach closely match those obtained from direct MCS for all cases. Like the previous example, the active Kriging approach deviates significantly from the benchmark results. Table 3 presents a comparison of the required number of NLTHA for the different approaches. This comparison provides observations, similar to the previous example, on the computational efficiency of the three different approaches for the SRA of the bridge pier.

5. Conclusions

An adaptive metamodeling approach for SRA of structures involving nonlinear seismic response approximation by incorporating active learning techniques and employing sparse Bayesian regression as the metamodeling technique is developed. The effectiveness of the proposed approach is demonstrated numerically using two realistic SRA problems involving NLTHA. The reliability results are compared with the existing Kriging-based active learning approach to assess the effectiveness of the proposed SRA approach. Based on the findings from the study, the following conclusions on the present research are made:

- The results clearly revealed the superiority of the proposed approach, as the predicted outcomes closely aligned with those obtained from the direct MCS technique. The number of actual function evaluations involving NLTHA and consequently the computational time is less than that of the existing active learning approach.
- The separate sparse Bayesian regression metamodels for each earthquake record avoid the need for prior distribution assumptions of seismic responses and capture nonlinear trends effectively. Thus, the proposed approach provides a more flexible and robust framework for more accurate prediction in SRA.
- Only one NLTHA is needed to add training data in each iteration. Thus, the proposed approach significantly reduces computational cost. This facilitates the achievement of good accuracy and much higher efficiency than the existing approach.

The fundamental steps of the proposed approach are generic, and it can be adapted to a wide range of structures and locations, replacing the mechanical model of the structure and generating ground motion data specific to the site under consideration. Thus, the proposed approach can be seamlessly applied to different types of structures, such as buildings, bridges, or offshore platforms, and in various geographical locations. The study can be further expanded for reliability analysis of nonlinear structures subjected to other types of stochastic dynamic loading, including wind, waves, blasts, etc.

CRediT authorship contribution statement

Atin Roy: Data curation, Formal analysis, Methodology, Software, Validation, Writing – original draft. **Subrata Chakraborty:** Conceptualization, Resources, Supervision, Writing – review & editing. **Sondipon Adhikari:** Resources, Supervision, Writing – review & editing.

Declaration of competing interest

The authors declare that they have no known competing financial interests or personal relationships that could have appeared to influence the work reported in this paper.

Data availability

Data will be made available on request.

References

[1] H.J. Pradlwarter, G.I. Schuëller, On advanced Monte Carlo simulation procedures in stochastic structural dynamics, Int. J. Non Lin. Mech. 32 (1997) 735–744, https://doi.org/10.1016/S0020-7462(96)00091-1.

[2] G.I. Schuëller, H.J. Pradlwarter, C.G. Bucher, Efficient computational procedures for reliability estimates of MDOF-systems, Int. J. Non Lin. Mech. 26 (1991) 961–974, https://doi.org/10.1016/0020-7462(91)90044-T.

[3] M. Xiong, Z. Chen, Y. Huang, Nonlinear stochastic seismic dynamic response analysis of submerged floating tunnel subjected to non-stationary ground motion, Int. J. Non Lin. Mech. 148 (2023) 104270, https://doi.org/10.1016/J.IJNONLINMEC.2022.104270.

[4] K. Porter, R. Kennedy, R. Bachman, Creating fragility functions for performance-based earthquake engineering, Earthq. Spectra 23 (2007) 471–489, https://doi.org/10.1193/1.2720892.

[5] P.E. Pinto, Reliability methods in earthquake engineering, Prog. Struct. Eng. Mater. 3 (2001) 76–85, https://doi.org/10.1002/PSE.64.

[6] N. Buratti, B. Ferracuti, M. Savoia, Response Surface with random factors for seismic fragility of reinforced concrete frames, Struct. Saf. 32 (2010) 42–51, https://doi.org/10.1016/J.STRUSAFE.2009.06.003.

[7] O.C. Celik, B.R. Ellingwood, Seismic fragilities for non-ductile reinforced concrete frames – role of aleatoric and epistemic uncertainties, Struct. Saf. 32 (2010) 1–12, https://doi.org/10.1016/J.STRUSAFE.2009.04.003.

[8] M. Fragiadakis, D. Vamvatsikos, M.G. Karlaftis, N.D. Lagaros, M. Papadrakakis, Seismic assessment of structures and lifelines, J. Sound Vib. 334 (2015) 29–56, https://doi.org/10.1016/J.JSV.2013.12.031.

[9] S. Ghosh, S. Ghosh, S. Chakraborty, Seismic fragility analysis in the probabilistic performance-based earthquake engineering framework: an overview, Int. J. Adv. Eng. Sci. Appl. Math. (13) (2017) 122–135, https://doi.org/10.1007/S12572-017-0200-Y, 2017 131.

[10] O.S. Kwon, A. Elnashai, The effect of material and ground motion uncertainty on the seismic vulnerability curves of RC structure, Eng. Struct. 28 (2006) 289–303, https://doi.org/10.1016/J.ENGSTRUCT.2005.07.010.

[11] P. Franchin, A. Lupoi, P.E. Pinto, M.I. Schotanus, Seismic fragility of reinforced concrete structures using a response surface approach, J. Earthq. Eng. 7 (2003) 45–77, https://doi.org/10.1142/S1363246903000961.

[12] O. Möller, R.O. Foschi, M. Rubinstein, L. Quiroz, Seismic structural reliability using different nonlinear dynamic response surface approximations, Struct. Saf. 31 (2009) 432–442, https://doi.org/10.1016/J.STRUSAFE.2008.12.001.

[13] J. Seo, L. Dueñas-Osorio, J.I. Craig, B.J. Goodno, Metamodel-based regional vulnerability estimate of irregular steel moment-frame structures subjected to earthquake events, Eng. Struct. 45 (2012) 585–597, https://doi.org/10.1016/J.ENGSTRUCT.2012.07.003.

[14] J. Seo, D.G. Linzell, Use of response surface metamodels to generate system level fragilities for existing curved steel bridges, Eng. Struct. 52 (2013) 642–653, https://doi.org/10.1016/J.ENGSTRUCT.2013.03.023.

[15] J. Park, P. Towashiraporn, Rapid seismic damage assessment of railway bridges using the response-surface statistical model, Struct. Saf. 47 (2014) 1–12, https://doi.org/10.1016/J.STRUSAFE.2013.10.001.

[16] S.K. Saha, V. Matsagar, S. Chakraborty, Uncertainty quantification and seismic fragility of base-isolated liquid storage tanks using response surface models, Probabilist. Eng. Mech. 43 (2016) 20–35, https://doi.org/10.1016/J.PROBENGMECH.2015.10.008.

[17] J.R. Gaxiola-Camacho, H. Azizsoltani, F.J. Villegas-Mercado, A. Haldar, A novel reliability technique for implementation of Performance-Based Seismic Design of structures, Eng. Struct. 142 (2017) 137–147, https://doi.org/10.1016/J.ENGSTRUCT.2017.03.076.

[18] C. Kim, S. Wang, K.K. Choi, Efficient response surface modeling by using moving least-squares method and sensitivity, AIAA J. 43 (2005) 2404–2411, https://doi.org/10.2514/1.12366.

[19] S. Ghosh, S. Chakraborty, Simulation based improved seismic fragility analysis of structures, Earthquakes Struct 12 (2017) 569–581, https://doi.org/10.12989/EAS.2017.12.5.569.

[20] N.D. Lagaros, M. Fragiadakis, Fragility assessment of steel frames using neural networks, Earthq. Spectra 23 (2007) 735–752, https://doi.org/10.1193/1.2798241.

[21] N.D. Lagaros, Y. Tsompanakis, P.N. Psarropoulos, E.C. Georgopoulos, Computationally efficient seismic fragility analysis of geostructures, Comput. Struct. 87 (2009) 1195–1203, https://doi.org/10.1016/j.compstruc.2008.12.001.

[22] S. Ghosh, A. Roy, S. Chakraborty, Support vector regression based metamodeling for seismic reliability analysis of structures, Appl. Math. Model. 64 (2018) 584–602, https://doi.org/10.1016/j.apm.2018.07.054.

[23] A. Roy, S. Chakraborty, Seismic reliability analysis of structures by an adaptive support vector regression-based metamodel, J. Earthq. Eng. (2023), https://doi.org/10.1080/13632469.2023.2242975.

[24] I. Gidaris, A.A. Taflanidis, G.P. Mavroeidis, Kriging metamodeling in seismic risk assessment based on stochastic ground motion models, Earthq. Eng. Struct. Dynam. 44 (2015) 2377–2399, https://doi.org/10.1002/EQE.2586.

[25] S. Ghosh, A. Roy, S. Chakraborty, Kriging metamodeling-based Monte Carlo simulation for improved seismic fragility analysis of structures, J. Earthq. Eng. 25 (2021) 1316–1336, https://doi.org/10.1080/13632469.2019.1570395.

[26] D.K.J. Lin, W. Tu, Dual response surface optimisation, J. Qual. Technol. 27 (1995) 34–39, https://doi.org/10.1080/00224065.1995.11979556.

[27] P. Towashiraporn, Building Seismic Fragilities Using Response Surface Metamodels, Georgia Institute of Technology, 2004. PhD thesis, https://search.proquest.com/openview/c9295fb2060f2854f76a5457a5db79b0/1?pq-origsite=gscholar&cbl=18750&diss=y. (Accessed 21 November 2021).

[28] S. Ghosh, S. Ghosh, S. Chakraborty, Seismic reliability analysis of reinforced concrete bridge pier using efficient response surface method–based simulation, Adv. Struct. Eng. 21 (2018) 2326–2339, https://doi.org/10.1177/1369433218773422.

[29] Y. Zhang, G. Wu, Seismic vulnerability analysis of RC bridges based on Kriging model, J. Earthq. Eng. 23 (2019) 242–260, https://doi.org/10.1080/13632469.2017.1323040.

[30] Y. Xiao, K. Ye, W. He, An improved response surface method for fragility analysis of base-isolated structures considering the correlation of seismic demands on structural components, Bull. Earthq. Eng. 18 (2020) 4039–4059, https://doi.org/10.1007/s10518-020-00836-w.

[31] V.U. Unnikrishnan, A.M. Prasad, B.N. Rao, Development of fragility curves using high-dimensional model representation, Earthq. Eng. Struct. Dynam. 42 (2013) 419–430, https://doi.org/10.1002/EQE.2214.

[32] I. Zentner, E. Borgonovo, Construction of variance-based metamodels for probabilistic seismic analysis and fragility assessment, Georisk Assess, Manag. Risk Eng. Syst. Geohazards. 8 (2014) 202–216, https://doi.org/10.1080/17499518.2014.958173.

[33] C.V. Mai, M.D. Spiridonakos, E.N. Chatzi, B. Sudret, Surrogate modelling for stochastic dynamical systems by combining Narx models and polynomial chaos expansions, Int. J. Uncertain. Quantification 6 (2016) 313–339, https://doi.org/10.1615/INT.J.UNCERTAINTYQUANTIFICATION.2016016603.

[34] A. Kundu, S. Ghosh, S. Chakraborty, A long short-term memory based deep learning algorithm for seismic response uncertainty quantification, Probabilist. Eng. Mech. 67 (2022) 103189, https://doi.org/10.1016/j.probengmech.2021.103189.

[35] C.G. Bucher, U. Bourgund, A fast and efficient response surface approach for structural reliability problems, Struct. Saf. 7 (1990) 57–66, https://doi.org/10.1016/0167-4730(90)90012-E.

[36] M.R. Rajashekhar, B.R. Ellingwood, A new look at the response surface approach for reliability analysis, Struct. Saf. 12 (1993) 205–220, https://doi.org/10.1016/0167-4730(93)90003-J.

[37] B. Echard, N. Gayton, M. Lemaire, AK-MCS: an active learning reliability method combining Kriging and Monte Carlo Simulation, Struct. Saf. 33 (2011) 145–154, https://doi.org/10.1016/j.strusafe.2011.01.002. (Accessed 10 June 2019).

[38] B. Richard, C. Cremona, L. Adelaide, A response surface method based on support vector machines trained with an adaptive experimental design, Struct. Saf. 39 (2012) 14–21, https://doi.org/10.1016/j.strusafe.2012.05.001. (Accessed 10 June 2019).

[39] Q. Pan, D. Dias, An efficient reliability method combining adaptive Support Vector Machine and Monte Carlo Simulation, Struct. Saf. 67 (2017) 85–95, https://doi.org/10.1016/j.strusafe.2017.04.006.

[40] J.M. Bourinet, Rare-event probability estimation with adaptive support vector regression surrogates, Reliab. Eng. Syst. Saf. 150 (2016) 210–221, https://doi.org/10.1016/j.ress.2016.01.023.

[41] S. Marelli, B. Sudret, An active-learning algorithm that combines sparse polynomial chaos expansions and bootstrap for structural reliability analysis, Struct. Saf. 75 (2018) 67–74, https://doi.org/10.1016/j.strusafe.2018.06.003.

[42] N.C. Xiao, M.J. Zuo, C. Zhou, A new adaptive sequential sampling method to construct surrogate models for efficient reliability analysis, Reliab. Eng. Syst. Saf. 169 (2018) 330–338, https://doi.org/10.1016/j.ress.2017.09.008.

[43] X. Li, C. Gong, L. Gu, W. Gao, Z. Jing, H. Su, A sequential surrogate method for reliability analysis based on radial basis function, Struct. Saf. 73 (2018) 42–53, https://doi.org/10.1016/j.strusafe.2018.02.005.

[44] K. Cheng, Z. Lu, Structural reliability analysis based on ensemble learning of surrogate models, Struct. Saf. 83 (2020) 101905, https://doi.org/10.1016/j.strusafe.2019.101905.

[45] A. Roy, S. Chakraborty, Support vector regression based metamodel by sequential adaptive sampling for reliability analysis of structures, Reliab. Eng. Syst. Saf. 200 (2020) 106948, https://doi.org/10.1016/j.ress.2020.106948.

[46] A. Roy, S. Chakraborty, Reliability analysis of structures by a three-stage sequential sampling based adaptive support vector regression model, Reliab. Eng. Syst. Saf. 219 (2022) 108260, https://doi.org/10.1016/j.ress.2021.108260.

[47] C. Ren, Y. Aoues, D. Lemosse, E. Souza De Cursi, Ensemble of surrogates combining Kriging and Artificial Neural Networks for reliability analysis with local goodness measurement, Struct. Saf. 96 (2022) 102186, https://doi.org/10.1016/j.strusafe.2022.102186.

[48] A. Roy, S. Chakraborty, S. Adhikari, Reliability analysis of structures by active learning enhanced sparse bayesian regression, J. Eng. Mech. 149 (2023) 04023024, https://doi.org/10.1061/jenmdt.emeng-6964.

[49] R. Teixeira, M. Nogal, A. O'Connor, Adaptive approaches in metamodel-based reliability analysis: a review, Struct. Saf. 89 (2021) 102019, https://doi.org/10.1016/j.strusafe.2020.102019.
[50] B.J. Bichon, M.S. Eldred, L.P. Swiler, S. Mahadevan, J.M. McFarland, Efficient global reliability analysis for nonlinear implicit performance functions, AIAA J. 46 (2008) 2459–2468, https://doi.org/10.2514/1.34321.
[51] M. Moustapha, S. Marelli, B. Sudret, Active learning for structural reliability: survey, general framework and benchmark, Struct. Saf. 96 (2022) 102174, https://doi.org/10.1016/J.STRUSAFE.2021.102174.
[52] Y. Xiao, F. Yue, X. Zhang, Seismic fragility analysis of structures based on adaptive Gaussian process regression metamodel, Shock Vib. 2021 (2021), https://doi.org/10.1155/2021/7622130.
[53] Y. Xiao, X. Zhang, F. Yue, M.M. Shahzad, X. Wang, B. Fan, Seismic fragility analysis of mega-frame with vibration control substructure based on dual surrogate model and active learning, Buildings 12 (2022) 752, https://doi.org/10.3390/buildings12060752.
[54] A.B. Jeddi, A. Shafieezadeh, J. Hur, J.G. Ha, D. Hahm, M.K. Kim, Multi-hazard typhoon and earthquake collapse fragility models for transmission towers: an active learning reliability approach using gradient boosting classifiers, Earthq. Eng. Struct. Dynam. 51 (2022) 3552–3573, https://doi.org/10.1002/EQE.3735.
[55] N.M. Newmark, A method of computation for structural dynamics, J. Eng. Mech. Div. 85 (1959) 67–94, https://doi.org/10.1061/JMCEA3.0000098.
[56] T.K. Datta, SEISMIC ANALYSIS OF STRUCTURES, John Wiley & Sons (Asia) Pte Ltd, Singapore, 2010.
[57] M.E. Tipping, Sparse Bayesian learning and the relevance vector machine, J. Mach. Learn. Res. 1 (2001) 211–244, https://doi.org/10.1162/15324430152748236.
[58] M.E. Tipping, A. Faul, Fast marginal likelihood maximization for sparse Bayesian models, in: C.M. Bishop, B.J. Frey (Eds.), Proc. 9th Int. Work. Artif. Intell. Stat., Proceedings of Machine Learning Research, Key West, FL, 2003, pp. 276–283, in: https://proceedings.mlr.press/r4/tipping03a.html. (Accessed 28 July 2023).
[59] K.-T. Fang, D.K.J. Lin, P. Winker, Y. Zhang, Uniform design: theory and application, Technometrics 42 (2000) 237–248, https://doi.org/10.1080/00401706.2000.10486045.
[60] S. Ghosh, S. Chakraborty, Probabilistic seismic hazard analysis and synthetic ground motion generation for seismic risk assessment of structures in the northeast India, Int. J. Geotech. Earthq. Eng. 8 (2017) 39–59, https://doi.org/10.4018/IJGEE.2017070103.
[61] D.M. Boore, Simulation of ground motion using the stochastic method, Pure Appl. Geophys. 160 (2003) 635–676, https://doi.org/10.1007/PL00012553, 2003 1603.
[62] F. McKenna, G. Fenves, M. Scott, B. Jeremic, OpenSees: open system for earthquake engineering simulation. http://opensees.berkeley.edu, 2016.
[63] J.B. Mander, M.J.N. Priestley, R. Park, Theoretical StressStrain model for confined concrete, J. Struct. Eng. 114 (1988) 1804–1826, https://doi.org/10.1061/(ASCE)0733-9445(1988)114:8(1804.
[64] B.D. Scott, R. Park, M.J.N. Priestley, Stress-strain behavior of concrete confined by overlapping hoops at low and high strain rates, J. Proc. 79 (1982) 13–27, https://doi.org/10.14359/10875.
[65] M. Menegotto, P.E. Pinto, Method of analysis for cyclically loaded R. C. Plane frames including changes in geometry and non-elastic behavior of elements under combined normal force and bending, in: Proc. IABSE Symp. Resist. Ultim. Deform. Struct. Acted by Well Defin, 1973, pp. 15–22. Loads, https://cir.nii.ac.jp/crid/1571980075471506816. (Accessed 14 September 2023).
[66] FEMA-356, Prestandard and Commentary for the Seismic Rehabilitation of Buildings, 2000.
[67] S.H. Kim, M.Q. Feng, Fragility analysis of bridges under ground motion with spatial variation, Int. J. Non Lin. Mech. 38 (2003) 705–721, https://doi.org/10.1016/S0020-7462(01)00128-7.